buildings

MDPI

Article

Distribution Features of Deviation and Determination of a Tolerance Method for Prefabricated Concrete Components

Hao Long [1,2], Xiaoyong Luo [1,3,*], Jinhong Liu [1] and Hongzhan Xiang [1]

[1] School of Civil Engineering, Central South University, Changsha 410000, China; longhao@hncu.edu.cn (H.L.)
[2] School of Civil Engineering, Hunan City University, Yiyang 413000, China
[3] Hunan Prefabricated Building Engineering Technology Research Center, Central South University, Changsha 410000, China
* Correspondence: csu-luoxy@csu.edu.cn

Abstract: According to the current standards for prefabricated buildings, the dimensional tolerances of components are usually determined by experience, lacking a theoretical basis. This work demonstrates the mathematical distribution of the dimensional deviations of precast concrete components by measuring their three-dimensional dimensions. Utilizing the Kolmogorov–Smirnov test, the cumulative distribution function of dimension deviations was evaluated. In response to the fact that the tolerance division principle of equal upper and lower tolerance thresholds for prefabricated components in existing standards does not match the distribution of actual measured deviations of the components, this paper proposed a method for determining the tolerance values of prefabricated components based on the process capability index. The association between the process capability index and the qualification rate was utilized to determine the process capability index at a specified guarantee rate, which, in turn, determines the tolerance threshold values for various components. The results indicate that the range of unqualified random variables for the dimensional geometric parameters of the prefabricated components did not show a significant difference, with all values between 0.99 and 1.02. The coefficients of geometric parameter variation were all less than 0.0061, and the component dimensional deviation adhered to the normal distribution. By linking the process capability index with the pass rate, a process capability index of 0.55 at a guarantee rate of 90% was determined, along with the tolerance for various components.

Keywords: prefabricated component; geometric parameter statistics; probability distribution; K-S test; process capability index; tolerance

check for updates

Citation: Long, H.; Luo, X.; Liu, J.; Xiang, H. Distribution Features of Deviation and Determination of a Tolerance Method for Prefabricated Concrete Components. *Buildings* **2023**, *13*, 1142. https://doi.org/10.3390/buildings13051142

Academic Editor: Ahmed Senouci

Received: 1 April 2023
Revised: 17 April 2023
Accepted: 23 April 2023
Published: 25 April 2023

Copyright: © 2023 by the authors. Licensee MDPI, Basel, Switzerland. This article is an open access article distributed under the terms and conditions of the Creative Commons Attribution (CC BY) license (https://creativecommons.org/licenses/by/4.0/).

1. Introduction

In China, the development of prefabricated buildings is an important direction for building structures, and it is conducive to the development of building industrialization [1]. Prefabricated buildings are structures constructed by transferring the primary structural components manufactured in a factory to a construction site and lifting them into place. Prefabrication shortens the time required for building, enables the realization of better architectural designs, and improves the construction quality [2,3]. Therefore, prefabricated buildings have been widely utilized throughout the world.

As applied in building construction, prefabricated components provide numerous benefits, while also limiting quality control. Considering that building components do not need to be created onsite, the quality of prefabricated components is crucial to the structural performance of prefabricated buildings [4]. Construction projects inevitably involve flaws in structural components [5]. These components can be either too large or too small, while their assembly can be problematic, resulting in joints that are too large, generating seepage issues [6]. The failure of precast concrete structures can occur if the dimensional quality of individual components does not comply with design codes [7]. Reworking to fix defects can

amount to 10% of the total costs in civil infrastructure projects [8], while the construction costs can reach 16% of the total project costs when the defects are fixed at the last stage [9].

The dimensional tolerance of prefabricated components refers to the permissible deviation between the component's actual size and its design value. Tolerance is crucial to the dimensional accuracy of prefabricated components. Existing dimensional tolerance control requirements for prefabricated components are present in numerous countries. The tolerances or variances suggested by domestic and international standards for prefabricated buildings and components are derived mostly from field experience and practice, rather than theoretical evaluation [10]. Currently, the values of tolerances and variances of prefabricated buildings vary by standards. The tolerance standards for diverse prefabricated structural systems, as well as dimensions and shapes, are inconsistent, which makes it difficult to evaluate whether prefabricated components meet a certain standard. Efficient tolerance analysis can significantly decrease the total amount of construction waste, increase productivity, and contribute to a leaner process [3,11]. Therefore, it is essential to determine the theoretical basis, the scope and evaluation criteria of prefabricated buildings, and the component tolerance in the construction industry.

According to the current standards applied to prefabricated buildings, the dimensional tolerances of the components are typically empirically determined, and this process lacks a theoretical basis. Therefore, this paper is based on our previous research [12] that proposes a method for obtaining information regarding the dimensions of prefabricated components using three-dimensional (3D) photogrammetry. Dimensional size deviation information was obtained from the dimensions of precast concrete components in China using 3D photogrammetry, and statistical tests were selected based on the characteristics of data distribution and variance. A method for determining the dimensional tolerance value of prefabricated components is proposed on the basis of the process capability index.

2. Geometric Feature Measurement of Prefabricated Components on Point Cloud

In current practice, the inspection of the dimensional variation of structural components mostly relies on classical measurements obtained by measuring tapes, leveling, or total stations, as shown in Figure 1. These methods are very time-consuming as regards the acquiring and interpreting of geometric data [5], and further, only a few points on the structure can be measured, meaning the resulting inspection may not fully reflect the actual, detailed condition of the complete object. Kim [13] claims that manual processes are unreliable, time-consuming, and expensive. For reliable communications between the various trades involved in a construction project, efficient and effective data storage and management systems are essential.



Figure 1. Traditional measurement methods.

2.1. Three-Dimensional Photogrammetry

In recent years, three-dimensional photogrammetry has gained popularity due to its ability to rapidly and precisely acquire range measurement data [14,15]. Due to these benefits, three-dimensional photogrammetry has been applied in the evaluation of the quality of civil structures [16,17]. The 3D laser photogrammetry technology used in this paper represents a novel measurement technique, considering its vision and reverse engineer-

ing characteristics. Under this process, we scanned the mark points on the prefabricated components from different angles, and then used the three-dimensional point normal principle to obtain the three-dimensional coordinates of each mark point, which were then converted into size values of the prefabricated components. As shown in Figure 2, the primary components of three-dimensional optical measurement equipment were coded as target points, non-coded marker points, and a measuring scale rod.

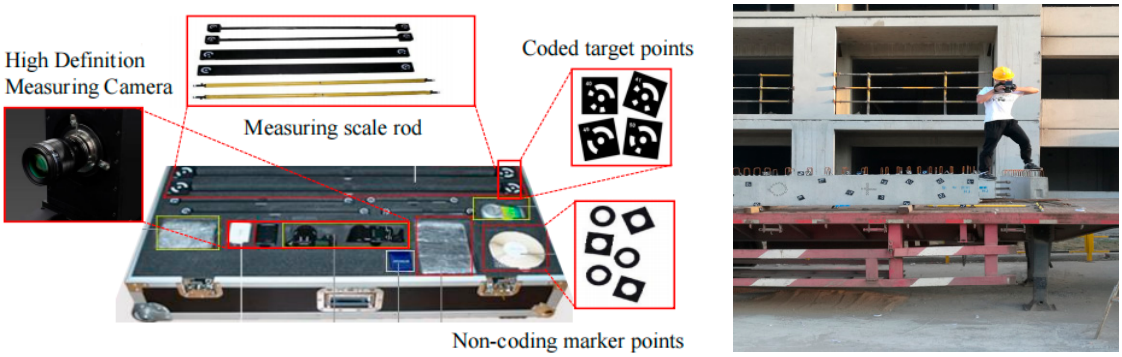


Figure 2. Three-dimensional photographic measuring instrument.

2.2. Three-Dimensional Point Cloud Data Form

In Figure 3, the original data of the 3D measurement are depicted as a point cloud, which shows the spatial distribution of the measured structure and a large number of points on the surface of the measured component. It contains the 3D coordinates, which are discrete and three-dimensional, as well as a large amount of data, and is arranged in a non-deforming manner. The point cloud data can be divided into three categories: the irrelevant point cloud contains the points that do not belong to the surface of the research component outside the point cloud of the research object, the second category is the surface noise caused by system errors, and the third category is the point cloud of the research object, which is referred to as the effective point cloud. There are numerous formats for presenting point cloud data, including las, pcd, ply, obj, and txt. Data processing in this paper was based on the C++ programming language. The PCL (Point Cloud Library) is a large, cross-platform, open-source C++ programming library developed on the basis of previous research pertaining to point clouds. It includes information relevant to point cloud acquisition, filtering, segmentation, registration, recognition, and surface reconstruction [18].

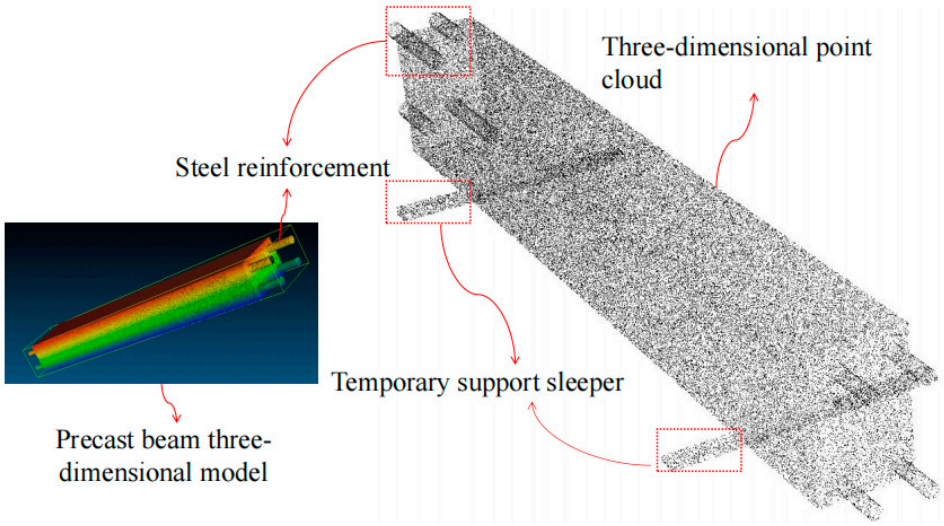


Figure 3. Three-dimensional point cloud of the precast beam component.

2.3. Processing of 3D Point Cloud Data for Prefabricated Components

When using point cloud data to obtain the three-dimensional dimensions of prefabricated components, a series of processing procedures is required to obtain the desired outputs from the raw point cloud data. The processing procedures comprise four main steps: (1) filtering noise reduction, (2) data registration, (3) data segmentation, and (4) geometric feature extraction, as shown in Figure 4. Data cleansing aims to remove noise from the raw point cloud data. Due to the complexity of actual construction site environments, the acquired point cloud data always contain various types of noise data, which are not useful to the intended project. In addition, various types of erroneous data also arise due to the limitations of specific sensors. Therefore, algorithms for noise removal are required to filter out useless data and only retain the data of interest. Data registration aims to align the multiple point clouds collected from different locations in a common coordinate system [5].

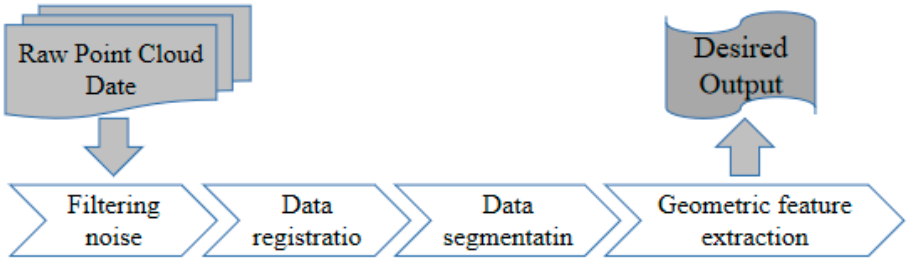


Figure 4. Typical processing procedures of point cloud data.

2.3.1. Filtering Noise Reduction

In the collection of point cloud data, taking into account the scanning angle, the scanning distance, the surface material of the object being measured, and the presence of obstacles and construction dust on the construction site, most three-dimensional point cloud models contain noise data. The presence of noise points can have an adverse effect on the extraction and measurement accuracy of the prefabricated component size characteristic values, so it is necessary to process the unrelated cloud data. The algorithm of cluster noise reduction usually involves setting thresholds to remove the isolated point clouds beyond a set distance from the main point cloud, and the rare point clouds that exceed a certain threshold set within the inner point cloud.

The part of the point cloud that is closest to the main point cloud, or is confused with the principal point cloud, belongs to the small-scale noise point, and is more difficult to remove. For dealing with this type of small-scale noise, there are three common filtering algorithms: medium-value filtering, average-value filtering, and Gauss filtering [19]. Among them, the Gauss filtration method employed in this article can more effectively remove the noise from the normal distribution, and this can redeem the authenticity of the data due to the occurrence of only small changes following noise reduction in the cloud, as shown in Figure 5.

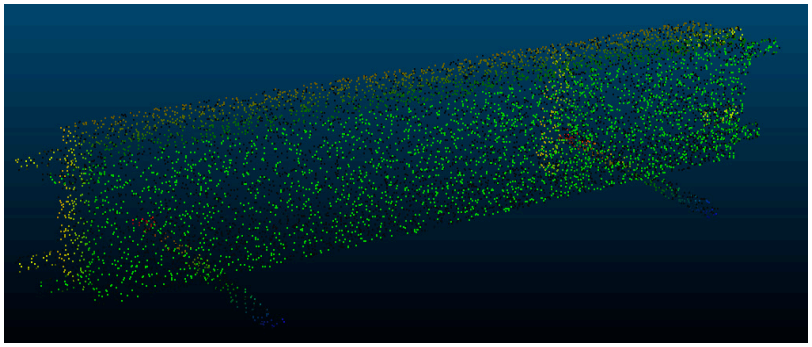


Figure 5. The component point cloud after noise reduction.

2.3.2. Data Registration and Data Segmentation

In order to ensure complete coverage of prefabricated components through the combination of point cloud data from multiple positions, it is essential to perform data registration, which aligns the point clouds in a common reference system. This process consists of two stages: coarse registration and fine registration [5]. During the coarse registration stage, a key point-based approach is employed. This approach involves the identification of key points in the point clouds using a specific point descriptor, followed by the calculation of the alignment between the two point clouds based on these key points. These descriptors serve to highlight significant features of each point, and subsequently reduce the original point cloud to a sparse set of key points. The resulting transformation matrix between the two point clouds is then computed based on the key points that overlap in both point clouds [20].

Data segmentation is a crucial step in the processing of point cloud data, as it allows for the identification and grouping of relevant segments or clusters that may correspond to different objects or geometric primitives. This process enables the efficient processing and analysis of the data. In addition, object recognition is essential for identifying specific objects in point cloud data, such as building components (walls, windows, and doors), which can be used to create detailed 3D models. There are several methodologies available for data segmentation, which can be classified into six categories, namely, clustering-based, edge-based [21], region-based [22], graph-based [23], model fitting-based [24], and hybrid approaches [24]. In this paper, we adopted a model fitting-based method to segment the point cloud data. This method involves fitting predefined models or shapes to the data, such as planes, spheres, or cylinders, and identifying the segments that match these shapes. This approach has been shown to be effective in various applications, including the recognition of building elements such as grouting sleeves, embedded components, and embedded bolts in point cloud data, which can aid in creating accurate and detailed 3D models of buildings.

2.3.3. Geometric Feature Extraction of Prefabricated Components

The density-based spatial clustering of applications with noise [25] (DBSCAN) algorithm was used to separate different concrete planes. Taking the point cloud data of the precast beam components in Figure 6 as an example, the tangent plane was fitted by the least-square method for point P and neighborhood points. The general expression of the plane equation is given by Equation (1):

$$z = -\frac{A}{C}x - \frac{B}{C}y - \frac{D}{C}(C \neq 0) \tag{1}$$

If we let $A_1 = -\frac{A}{C}$, $A_2 = -\frac{B}{C}$, $A_3 = -\frac{D}{C}$ and substitute it into Equation (1), this yields:

$$z = A_1 x + A_2 y + A_3 \tag{2}$$

The least-squares equation for k neighborhood points is:

$$S = \sum^{k} (y_i - z)^2 \tag{3}$$

In order to minimize S,

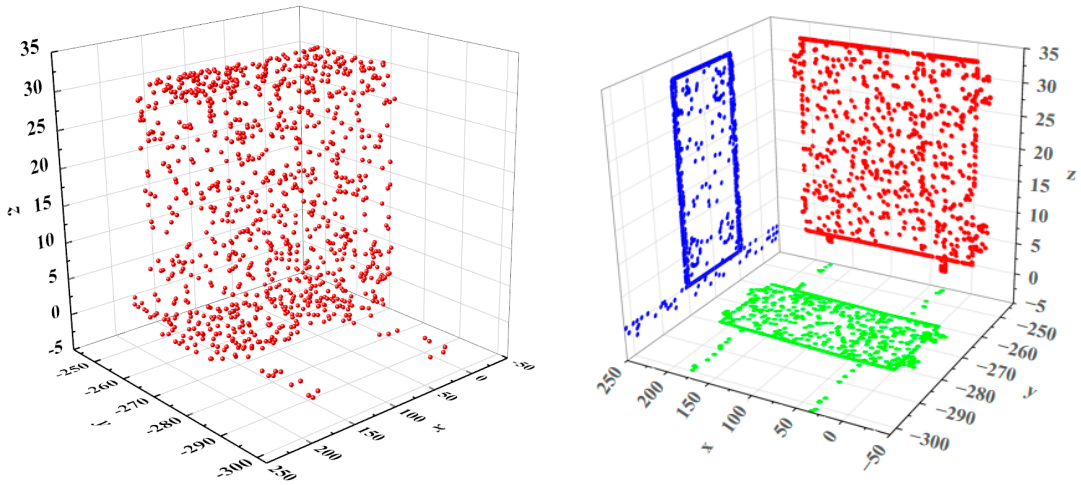
$$\frac{\partial S}{\partial A_k} = 0,\ k = 1, 2, 3 \tag{4}$$

$$\begin{cases} \sum_{i=1}^{k} 2(y_i - A_1x - A_2y - A_3)x = 0 \\ \sum_{i=1}^{k} 2(y_i - A_1x - A_2y - A_3)y = 0 \\ \sum_{i=1}^{k} 2(y_i - A_1x - A_2y - A_3) = 0 \end{cases} \tag{5}$$

Rewritten into a matrix form, this yields:

$$\begin{vmatrix} \sum x_i^2 & \sum x_i y_i & \sum x_i \\ \sum x_i y_i & \sum y_i^2 & \sum y_i \\ \sum x_i & \sum y_i & n \end{vmatrix} \begin{bmatrix} A_1 \\ A_2 \\ A_3 \end{bmatrix} = \begin{bmatrix} \sum x_i z_i \\ \sum y_i z_i \\ \sum z_i \end{bmatrix} \tag{6}$$

The parameters A_1, A_2, A_3 can be obtained by solving Equation (6), and the plane equation can be obtained by substituting it into Equation (3).



(**a**) Original point cloud data (**b**) Plane point cloud data

Figure 6. Dimension projection of the precast beam component.

It can be seen from Figure 6 that the point cloud projected onto the plane has good effectiveness. Using the geometric properties of the prefabricated components to complete the dimensional reduction of the data, the size information of the components can be obtained in a simple manner.

2.4. Three-Dimensional Measurement Accuracy Analysis

In order to evaluate the accuracy of the three-dimensional photogrammetry system, the root mean square error (RMSE) [26] was used to measure the difference between the values yielded by different measurement systems. RMSE is often used to describe the accuracy of features. If the measurement error and the quality of the estimated features are acceptable, a lower RMSE value will mean a higher accuracy. The accuracy of the three-dimensional measurement method was evaluated using Equation (7):

$$RMSE = \sqrt{\frac{\sum_{i-1}^{n}(x - \overline{x})^2}{n}} \tag{7}$$

where x represents each value in the dataset, $\overline{x}$ represents the average of all values in the dataset, and n represents the number of datasets.

The difference between a traditional measurement and photogrammetry is shown in Table 1. The RMSE value of photogrammetry was 3.31 mm, and that of steel ruler

measurement was 10.86 mm. The error of photogrammetry was within the range of 0.01 mm. Compared with traditional measurement approaches, the error yielded by photogrammetry was small. Considering the non-planar characteristics of concrete components and the low manufacturing accuracy of the components themselves, it is difficult to completely avoid errors. Therefore, the accuracy of the detection system can meet the actual engineering requirements, on the premise of achieving accuracy in concrete size detection.

Table 1. RMSE values of the traditional measurement method and the photogrammetric method (unit: mm).

Items	Design Value	Steel Tape		Photogrammetry		x^2	x^2
		Measurement	Deviation	Measurement	Deviation		
1	2830	2833	−3	2831.86	−1.86	9	3.46
2	400	402	−2	400.82	−0.82	4	0.67
3	410	413	−3	412.03	−2.03	9	4.12
4	2535	2539	−4	2537.08	−2.08	16	4.33
5	500	503	−3	502.07	−2.07	9	4.28
6	520	523	−3	520.67	−0.67	9	0.45
7	6630	6633	−3	6629.84	0.16	9	0.02
8	2600	2598	2	2599.24	0.76	4	0.58
9	240	238	2	240.65	−0.65	4	0.42
10	4350	4355	−5	4346.06	3.94	25	15.52
11	3930	3933	−3	3926.95	3.05	9	9.30
12	2900	2905	5	2898.23	−1.77	25	3.13
13	3200	3204	4	3203.76	−0.34	16	0.12
14	240	242	2	240.18	−0.24	4	0.06
		$\sum$				152	46.46
RMSE		$\sqrt{\sum}/14$		$\sqrt{\sum}/11$		10.86	3.31

3. Size Deviation and Distribution Characteristics of Precast Concrete Components

3.1. Measurement Object

Our measurements of component size deviation were mainly derived from the northern region, mainly Zhengzhou, China, and the southern region, mainly Changsha. The measurement objects included four prefabricated component companies, who mainly develop components of prefabricated building structures: beams, columns, wall slabs, and prefabricated composite floor slabs. Each type of component was randomly selected by a random sampling method. The number of survey samples is shown in Table 2.

Table 2. The number of precast concrete measurement samples.

Project	Structure Type	Sample Number			
		Beam	Column	Wall Slab	Composite Floor Slab
Zhongmin Zhuyou Co., Ltd., Changsha, China	Precast frame	62	66	102	87
Hydropower Eight Bureau Co., Ltd., Changsha, China	Precast frame shear wall	54	129	84	96
Sanneng Integrated Housing Co., Ltd., Changsha, China	Precast shear wall	76	94	64	111
China Construction Seventh Bureau., Henan, China	Precast frame shear wall	103	85	121	107

3.2. Size Deviation Correlation Test

The design dimensions of the components used here are different, and the dimensional variability was used to evaluate and analyze whether the dimensional deviations of the

components produced by different factories are similar. The geometrical uncertainty is represented by a random variable K_a [27], and can be calculated via:

$$K_a = \frac{a}{a_K} \tag{8}$$

where a is the actual value of the component size, and a_K is the design value of the component size.

Component dimensions are regarded as independent random variables, while components of the same type produced by the same enterprise are regarded as a matrix, and samples of $n > 50$ capacity were used to analyze this matrix. The level of variation in the geometric dimensions of the component is represented by the weighted average value of the geometric dimensions of the same type of component. The statistical parameters of the random variables with uncertain geometric dimensions can be expressed as:

$$\mu_{K_a} = \frac{\sum_{i=1}^{n} n_i \mu_{K_{A_i}}}{\sum_{i=1}^{n} n_i} \tag{9}$$

$$\delta_{K_a} = \frac{\sum_{i=1}^{n} n_i \delta_{K_{A_i}}}{\sum_{i=1}^{n} n_i} \tag{10}$$

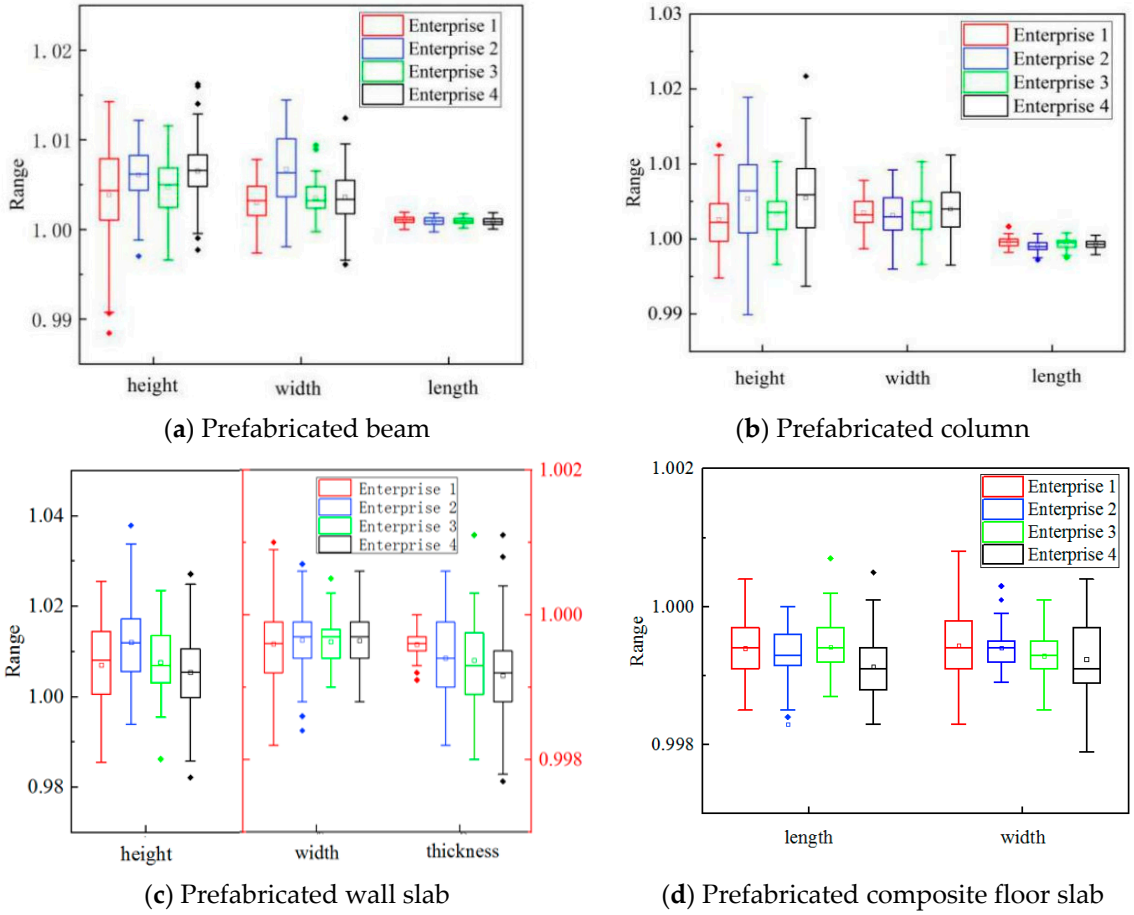
where n_i is the sample capacity of the geometric characteristic value of the same type of component, μ_{K_i} is the average of n_i, and δ_{K_i} is the coefficient of variation, while the statistical parameters of the uncertain random variable of the component's geometric parameters can be obtained using Equations (9) and (10), and the results are shown in Table 3.

Table 3. Summary of samples' statistical results.

Type	Project	Enterprise 1		Enterprise 2		Enterprise 3		Enterprise 4	
		μ_k/mm	δ_k	μ_k/mm	δ_k	μ_k/mm	δ_k	μ_k/mm	δ_k
Beam	Length	1.0011	0.0004	1.0009	0.0005	1.0010	0.0004	1.0065	0.0034
	Width	1.0030	0.0023	1.0060	0.0038	1.0035	0.0018	1.0036	0.0030
	Height	1.0039	0.0056	1.0061	0.0032	1.0047	0.0031	1.0065	0.0034
Column	Length	0.9996	0.0007	0.9991	0.0007	0.9993	0.0007	0.9993	0.0006
	Width	1.0035	0.0019	1.0031	0.0029	1.0033	0.0029	1.0039	0.0032
	Height	1.0026	0.0040	1.0053	0.0061	1.0033	0.0029	1.0055	0.0056
Wall slab	Height	0.9996	0.0002	0.9994	0.0005	0.9994	0.0006	0.9992	0.0006
	Width	0.9996	0.0005	0.9997	0.0004	0.9996	0.0003	0.9997	0.0004
	Thickness	1.0071	0.0093	1.0121	0.0089	1.0026	0.0070	1.0054	0.0084
Composite floor slab	Length	0.9994	0.0006	0.9994	0.0003	0.9993	0.0003	0.9992	0.0005
	Width	0.9994	0.0004	0.9993	0.0003	0.9994	0.0004	0.9991	0.0004

The maximum values, minimum values, upper and lower quartiles, and average values of the geometric parameters of each enterprise's components were compared, as shown in Figure 7. The diversity amongst the range of components produced by different manufacturers was not great, as all were in the range of 0.99~1.02. Here, the abnormal points of beam components accounted for 3.4% of the total, the abnormal points of column components accounted for 0.8% of the total, the abnormal points of wall slabs accounted for 3.5% of the total, and the abnormal points of laminated floors accounted for 1.2% of the total. There was less variability in terms of bias. The partial volume of the box indicates the

degree of data dispersion in the group; in this case, the K_A value of the box was lower and fluctuated less.



(**a**) Prefabricated beam (**b**) Prefabricated column

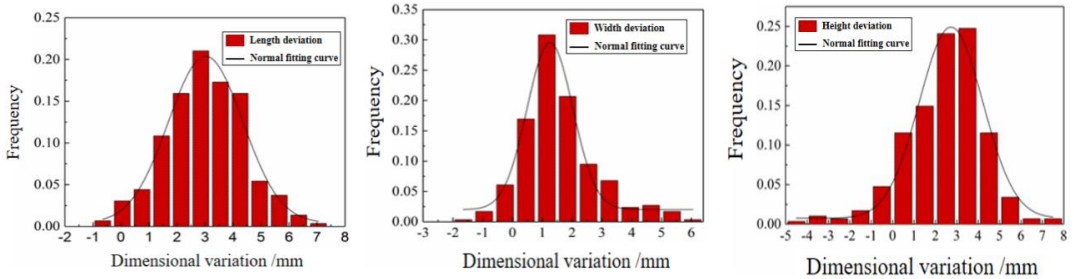
(**c**) Prefabricated wall slab (**d**) Prefabricated composite floor slab

Figure 7. Geometric uncertainty box line diagram of prefabricated components.

Table 3 compares the dimensional variation coefficients of similar components from different manufacturers. The uncertainty values of the transverse dimensions of components manufactured by various enterprises were all less than one, indicating negative deviations, whereas the dimensions of longitudinal components were all greater than one, indicating positive deviations. The size deviation of similar prefabricated components manufactured by the same company was not significant, and the measured data were reliable. The size of prefabricated components is largely determined by the manufacturers. The coefficients of variation were all less than 0.0094, indicating that the variation was small. The size characteristics of similar components manufactured by different companies were the same.

3.3. Size Deviation Distribution Characteristics of Precast Concrete Components

Since there was no statistically significant difference in the size deviation of similar components produced by different companies, this factor was used to illustrate the general size deviation of the prefabricated components, and the distribution law of the size deviation of the prefabricated components was analyzed using a histogram. A histogram can be used to determine the total probability density. The abscissa of the histogram represents the group median, and the ordinate is the measured frequency. As illustrated in Figures 8–11, the histograms were formed using the deviation value as the abscissa and the observed frequency as the ordinate. The histograms have a peak in the center that drops away on both sides, and a fitted curve fits to the graph, showing the Gaussian distribution function.

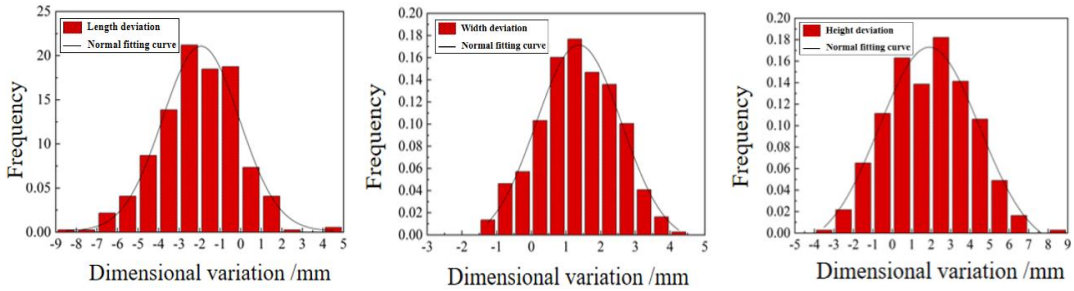


(**a**) Length deviation ($\mu = 3.022, \sigma = 1.910$)

(**b**) Width deviation ($\mu = 1.568, \sigma = 1.570$)

(**c**) Height deviation ($\mu = 2.449, \sigma = 3.272$)

Figure 8. Dimensional deviation distribution of the prefabricated beam components.

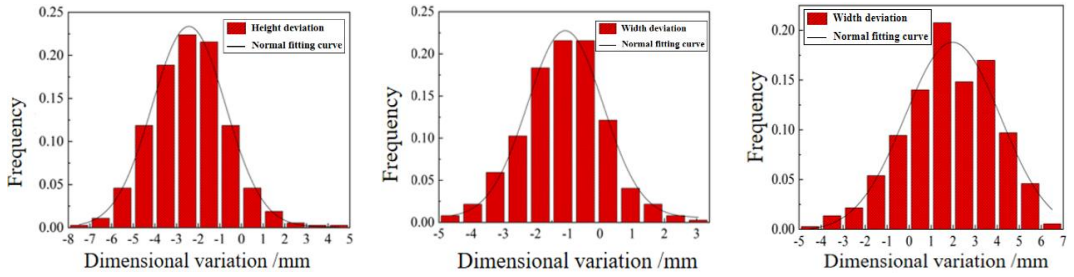


(**a**) Length deviation ($\mu = -2.050, \sigma = 3.742$)

(**b**) Width deviation ($\mu = 1.336, \sigma = 1.209$)

(**c**) Height deviation ($\mu = 1.883, \sigma = 4.344$)

Figure 9. Dimensional deviation distribution of the prefabricated column components.

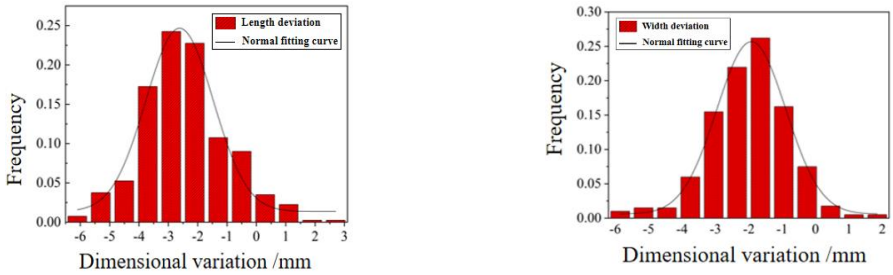


(**a**) Height deviation ($\mu = -2.390, \sigma = 2.911$)

(**b**) Width deviation ($\mu = -1.125, \sigma = 1.570$)

(**c**) Thickness deviation ($\mu = 1.807, \sigma = 4.134$)

Figure 10. Size deviation distribution of the prefabricated wall slab components.



(**a**) Length deviation ($\mu = -2.436, \sigma = 2.215$)

(**b**) Width deviation ($\mu = -2.023, \sigma = 1.428$)

Figure 11. Size deviation distribution of the composite floor slabs.

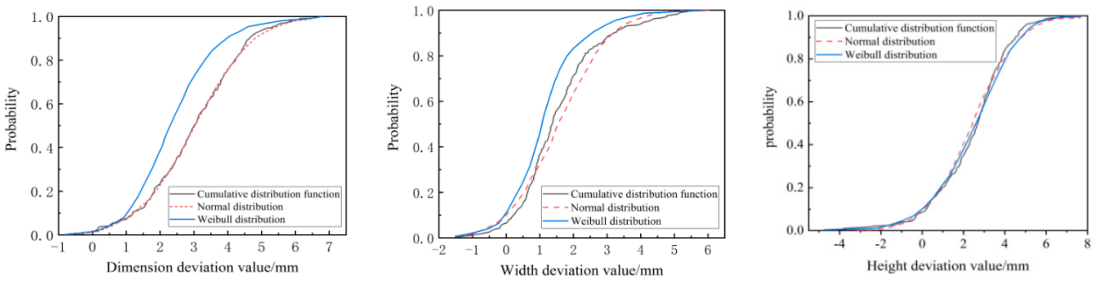
3.4. Prefabricated Component Size Deviation Goodness of Fit Test

The Kolmogorov–Smirnov test (K-S test) [28] was used to compare two samples (two-sample K-S test) in terms of whether they were drawn from the same distribution (the null hypothesis) [29]. Suppose that $X_1, X_2, \cdots, X_n$ and $Y_1, Y_2, \cdots, Y_n$ are two different samples: whether the two samples belong to the same population depends on the test statistic D value. The D value is defined as:

$$D = \max|S_X(x) - S_Y(x)| \tag{11}$$

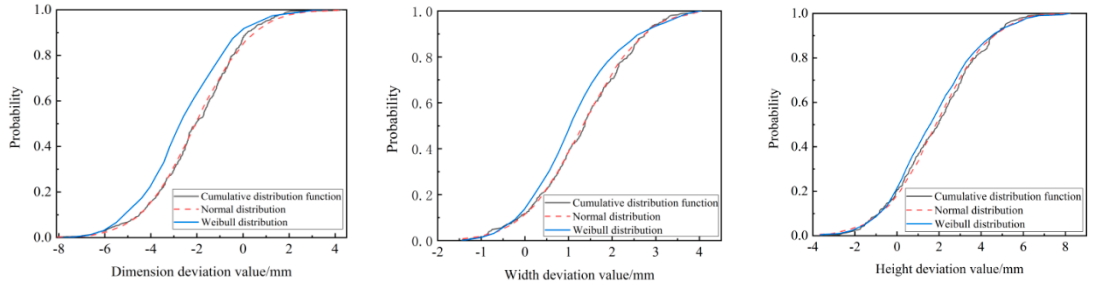
where $S_X(x)$ and $S_Y(x)$ are the cumulative distribution functions of the two samples.

If the D is small, it can be assumed that the two samples are from the same population. Considering the general applicability of the normal distribution to random variables and the universal significance of Weibull theory to the concrete size effect [30,31], the normal distribution and the Weibull distribution were used to compare the size deviation of the prefabricated components. The cumulative distribution function curves fitting different component size deviations are shown in Figures 12–15. The Weibull cumulative distribution function curve and the normal distribution function curve showed similar trends to that in the cumulative distribution function curve of the component dimension deviation. Intuitively, the cumulative distributions of the length deviation and the width deviation fit better with the normal distribution, with a significant difference from the Weibull distribution. The Weibull cumulative distribution and the normal cumulative distribution function curves were in good agreement as regards the deviation distributions of height, size, and wall thickness.



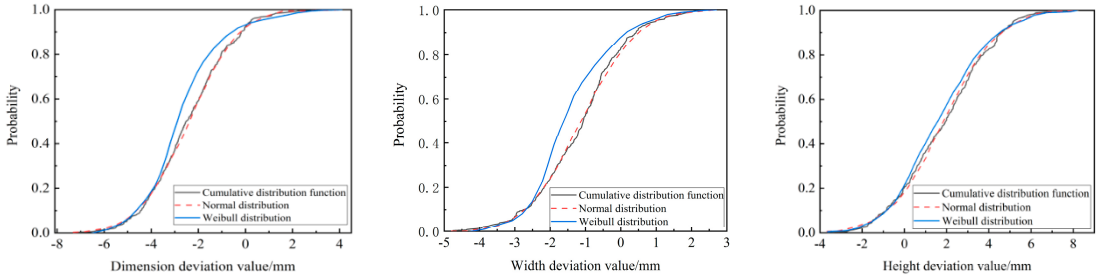
(**a**) Length deviation (**b**) Width deviation (**c**) Height deviation

Figure 12. Cumulative distribution function of dimension deviation of the prefabricated beam.



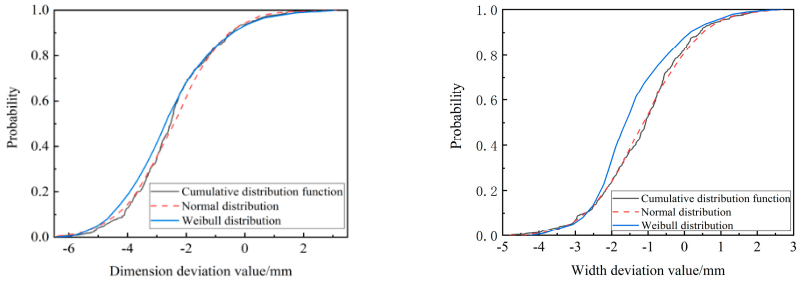
(**a**) Length deviation (**b**) Width deviation (**c**) Height deviation

Figure 13. Cumulative distribution function of dimension deviation of the prefabricated column.



(**a**) Height deviation (**b**) Width deviation (**c**) Thickness deviation

Figure 14. Cumulative distribution function of dimension deviation of the prefabricated column.



(**a**) Length deviation (**b**) Width deviation

Figure 15. Cumulative distribution function of dimension deviation of the composite floor slab.

In order to accurately compare and determine the optimal distribution, it is necessary to further calculate the maximum absolute deviation between the theoretical distribution function and the empirical distribution function, along with the probability of making the first type of error. The results are shown in Table 4, where, according to Equation (10), the values were calculated based on the Kolmogorov distribution. Among the two distributions, the normal distribution showed the smallest absolute maximum value of D and the smallest p-value. If the significance level of 0.05 is used, the fitting effects of both the normal and Weibull distributions were acceptable, with the latter obviously obeying the former, indicating that the dimensional deviation of the prefabricated components met the null hypothesis and conformed to normal distribution.

Table 4. Prefabricated component size deviation K-S test results.

Type	Project	Normal Distribution		Weibull Distribution	
		D	p	D	p
Beam	Length	0.038	0.592	0.213	0.039
	Width	0.077	0.187	0.098	0.028
	Height	0.044	0.331	0.052	0.311
Column	Length	0.073	0.429	0.189	0.033
	Width	0.098	0.373	0.167	0.048
	Height	0.031	0.333	0.094	0.309
Wall slab	Height	0.055	0.419	0.193	0.037
	Width	0.061	0.380	0.313	0.018
	Thickness	0.035	0.377	0.051	0.293
Composite floor slab	Length	0.087	0.199	0.199	0.038
	Width	0.019	0.211	0.227	0.031

4. Tolerance Analysis Theory of Prefabricated Building Components

4.1. Standard Tolerances for Prefabricated Concrete Component

According to Tolerances for Building Structures: DIN 18202-1997 [32] and Tolerances in Building Construction—Buildings: DIN 18202-2005 [33], the tolerance limits allowed for German prefabricated building components are shown in Table 5. From 1997 to 2005, the production capacity of prefabricated building components in Germany continuously improved, and the permitted tolerance limits have become more and more stringent.

Table 5. Allowable tolerance values in German standards.

Name	Item	Allowable Tolerance (mm)				
		<3 m	**3~6 m**	**6~15 m**	**15~30 m**	**>30 m**
Tolerances for Building Structures (DIN 18202-1997)	<3 m		±16	±20	±24	±30
	±12		±16	±20	±30	±30
	±16		±20	±24	±30	/
	±16	±20	±20	±30	/	/
	Hole Size	±12	±16	/	/	/
Tolerances in building construction—Buildings (DIN 18202-2005)	Plane Size	±10	±12	±20	±24	±30
	Height Dimension	±10	±16	±20	±30	±30
	Plane Clearance	±12	±16	±24	±30	/
	Vertical Clearance	±10	±12	/	/	/
	Hole Size	±8	±10	/	/	/

Unlike the German DIN 18202-2005, which stipulates the tolerance allocation method with equal positive and negative tolerance values, the European Harmonized Standard for Common Rules for Precast Concrete Products: EN 13369-2008 [34], stipulates tolerance limits with unequal positive and negative tolerances (in Table 6); for example, a tolerance of −5–10 mm is allowed for the length of precast beams (<1500 mm). In contrast, the US PCI Precast and Prestressed Concrete Control Manual: MNL-135-00 [35], uses partial non-integer system tolerances. For example, the tolerance limit for prefabricated columns of less than 3 m in height is ±12.7 mm, stating a more precise tolerance interval.

Table 6. Allowable tolerances under ACI 117-2010 and MNL-135 for component dimensions.

Name	Item		Allowable Tolerance (mm)			
			<3 m	**3–6 m**	**6–12 m**	**>12 m**
Specifications and Material Descriptions for Concrete Construction Tolerances (ACI 117-2010)	Wall slabs	Length	±3	−5–3	±6	±1.5 per 3 m
		Width	±6	−5–3	±6	±1.5 per 3 m
		Thickness			−3–6	
	Beam	Length			±19	
		Width			±6	
		Thickness			±6	
PCI Precast and Prestressed Concrete Control Manual (MNL-135)	Column	Length			±13	
		Width			±6	
		Thickness			±6	
	Floor	Length			±13	
		Width			±6	
		Thickness			±6	
	Wall slabs	Length			±13	
		Width			±6	
		Thickness			−3–6	
	Beam	Length			±25	
		Width			−6–10	
		Thickness			−6–13	

China has also developed a number of specifications and standards, the most important of which are the Technical Specification for Precast Concrete Structures: JGJ 1-2014 [36], the Code for Quality Acceptance of Concrete Structure Construction: GB/T 50204-2015 [37], and the Technical Standard for Prefabricated Buildings with Concrete Structure: GB/T 51231-2016 [38]. The tolerances permitted under Chinese Standards and Norms are shown in Table 7.

Table 7. Allowable tolerances under Chinese Standards and Norms.

Name	Item		Allowable Tolerance (mm)
Code for Quality Acceptance of Concrete Structure Construction (GB/T 50204-2015)	Length	Floor slab, beam, column, truss, wall slab	±5 (<12 m) ±10 (12~18 m) ±4
	Width, Height (Thickness)	Floor slab, beam, column, truss, wall slab	±5 ±4
Precast Concrete Construction Technique Standard (GB/T 51231-2016).	Length	Floor slab, beam, column, truss	±5 (<12 m) ±10 (12~18 m)
	Width, Height (Thickness)	Floor slab, beam, column, truss	±5
	Height Width Thickness	Wall slab	±4 ±4 ±3
Technical Specification for Precast Concrete Structures (JGJ 1-2014)	Length	Floor slab, beam, column, truss section size Wall slab	±5 (<12 m) ±10 (12~18 m) ±4
	Width, Height (Thickness)	Beam, plate, column, truss section size Wall slab height and thickness	±5 ±3

Currently, various standards set different values for the tolerances and variations relevant to prefabricated buildings. According to the German standard DIN 18203-1997, the tolerance for prefabricated components smaller than 3 m in length is 12 mm, whereas the tolerance for prefabricated wall slabs and beams is 5 to 10 mm under the Chinese National Standard GB/T50204-2015. Since the recommended tolerance and deviation values for prefabricated buildings vary between different standards, design, production, construction, and approval are complicated. The tolerance standards set for diverse prefabricated structural systems, dimensions, and shapes are inconsistent, which makes it difficult to evaluate whether prefabricated components meet a certain standard. In the construction sector, it is crucial to determine the theoretical basis, range, and evaluation criteria of tolerances for prefabricated buildings and components.

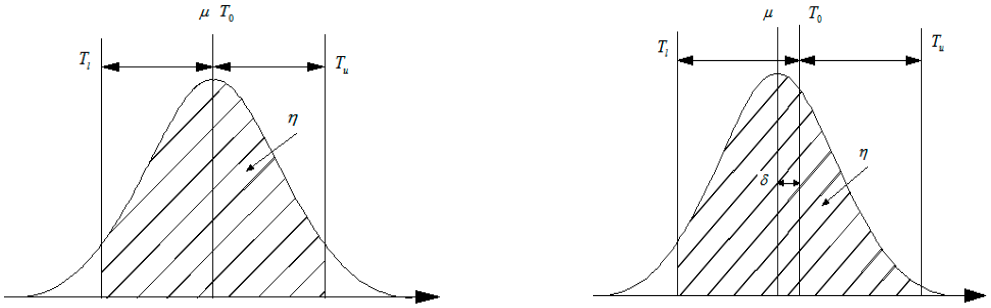
4.2. Theoretical Model of Dimensional Tolerance

The process capability index is used in manufacturing to determine the ability of a manufacturing process to ensure steady-state product quality [39]. Prefabricated components also have the same properties as machinery-manufactured products [40], and methods for their quality control may also be based on the process capability index. The process capability index can be used to quantify the quality compliance rate and process level, reflecting the process capability based on technical requirements (e.g., quality and size). The index is illustrated in Equation (12):

$$C_p = \frac{T_u - T_l}{6\sigma} = \frac{T}{6\sigma} \tag{12}$$

where C_p indicates the process capability index, T_u, T_l indicate the upper and lower tolerance limits, respectively, σ indicates the standard deviation, and T is the tolerance.

There are two main types of process capability indices: those that coincide with the distribution center, as shown in Figure 16a, and those that do not coincide with the distribution center, as shown in Figure 16b.



(**a**) The center of tolerance overlaps with the center of the mean.

(**b**) The center of tolerance does not overlap with the center of the mean.

Figure 16. Schematic diagram of tolerance center and dimension center.

According to the statistical analysis of the prefabricated component size, the center of the component size distribution does not coincide with the center value required by the specification. When the distribution center does not coincide with the tolerance center, the actual process capability index, C_{pk}, is calculated according to Equation (13), and δ is the deviation of the distribution center from the specification center. When the process capability index, C_{pk}, and the dimensional distribution center, μ, are known, the upper and lower tolerance limits of the prefabricated component can be calculated:

$$C_{pk} = \frac{T}{6\sigma}(1-\delta) = \frac{T_u - T_l}{6\sigma}\left(1 - \frac{|\mu - (T_u + T_l)/2|}{(T_u - T_l)/2}\right) \tag{13}$$

4.3. Process Capability Index and Qualification Rate

The process capability index actually reflects the qualification rate. The prefabricated component size satisfies the normal distribution, $N(\mu, \sigma^2)$, and the qualification rate, η, can be expressed as:

$$\eta = \int_{T_l}^{T_u} N(\mu, \sigma^2) = P(T_l \le X \le T_u) = P\left(\frac{T_l - \mu}{\sigma} \le \frac{X - \mu}{\sigma} \le \frac{T_u - \mu}{\sigma}\right) = \Phi\left(\frac{T_u - \mu}{\sigma}\right) - \Phi\left(\frac{T_l - \mu}{\sigma}\right) \tag{14}$$

where $\Phi()$ in Equation (14) denotes the cumulative distribution function of the standard normal distribution. Assume that:

$$d = (T_u - T_l)/2 \tag{15}$$

Then,

$$T_u = T_0 + d \tag{16}$$

$$T_l = T_0 - d \tag{17}$$

Substituting Equations (15)–(17) into Equation (14) yields:

$$\eta = 1 - \Phi\left(\frac{T_0 + d - \mu}{\sigma}\right) - \Phi\left(\frac{T_0 - d - \mu}{\sigma}\right) = 1 - \Phi\left(-\frac{d + (\mu - T_0)}{d} \times \frac{d}{\sigma}\right) - \Phi\left(-\frac{d - (\mu - T_0)}{d} \times \frac{d}{\sigma}\right) \tag{18}$$

Assuming that $\delta = \frac{\mu - T_0}{d}$, $\lambda = \frac{\sigma}{d}$ can be substituted into Equation (18):

$$\eta = 1 - \Phi\left(-\frac{1+\delta}{\lambda}\right) - \Phi\left(-\frac{1-\delta}{\lambda}\right) \tag{19}$$

Obviously, η and δ are symmetric functions, so Equation (19) can be transformed into:

$$\eta = 1 - \Phi(-\frac{1+|\delta|}{\lambda}) - \Phi(-\frac{1-|\delta|}{\lambda}) \tag{20}$$

Substituting $T_0 = (T_u + T_l)/2$, $d = (T_u - T_l)/2$, $\delta = \frac{u-T_0}{2}$, and $\lambda = \frac{\sigma}{d}$ into Equation (13) demonstrates the relationship between the qualification rate and the process capability index, C_{pk} [41], as shown in:

$$\eta = 1 - \Phi(-3C_{pk}) - \Phi(-3C_{pk}(\frac{1+|\delta|}{1-|\delta|})) \tag{21}$$

MATLAB iteration can be used to derive different process capability indices and qualification rates, as well as their relationships. As shown in Figure 17, the shape of the curve of the passing rate varied with the process capability index, and was related to the magnitude of the process capability index. Equation (21) shows that η has an extreme value when $\delta = 0$. When $C_{pk} < 1/3$, the pass rate curve is convex, as indicated by the shape in Figure 13 when $C_{pk} = 0.3$; when $1/3 < C_{pk} < 0.5605$, there are two minimal values of η, and the pass rate reaches a minimum near the limit of $\pm\delta$ before trending sharply upward to $\eta = 1$, while there is an extreme value of the interval at $\delta = 0$, as in $C_{pk} = 0.4$ in Figure 17. When $C_{pk} > 0.5605$, the η curve is concave and has only one minimal value, while when $\delta = 0$, the minimal value is equal to the pass rate corresponding to C_{pk}. Table 8 shows the minimum value of the corresponding pass rate when $C_{pk} > 1/3$ and the extreme value when $\delta = 0$.

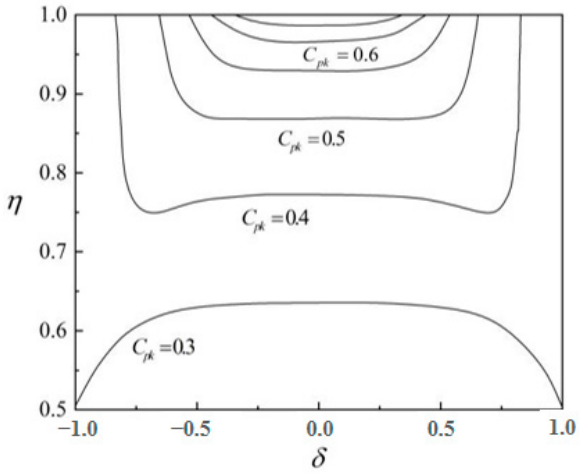


Figure 17. Relationship between the work process capability index and the qualification rate.

Table 8. The minimum qualification rates corresponding to process capability index values.

Process Capability Index	Minimum Qualification Rate	Qualification Rate of the Distribution Center's Deviation
C_{pk}	η_{min}	$\eta_{\delta=0}$
1/3	0.5	0.6827
0.4	0.7463	0.7699
0.5	0.8653	0.8664
0.55	0.901	0.9011
0.5605	0.9073	0.9073
0.6	0.9281	0.9281
1	0.9973	0.9973
1.3333	0.9999	0.9999
1.6667	1	1
2	1	1

4.4. Tolerance Threshold of Prefabricated Components Based on the Process Capability Index

According to the statistics regarding the dimensional deviation of prefabricated components, the qualification rates of dimensional deviation of the prefabricated components under the tolerance thresholds specified in the Chinese Technical Standards for prefabricated Concrete Buildings are shown in Table 9. There is currently no consensus on the allowable tolerance requirements for the production and construction of components in prefabricated buildings, and the standards are not systematic, lacking clear criteria and methods for determining tolerances. Existing tolerance determination is based on engineering experience, but it lacks research on tolerance control theory and probability statistics analysis. According to the standard tolerance threshold, except for cases when the height deviation of a prefabricated wall slab is less than 90%, the qualification rates of dimensional deviation of other components were higher than 90%. The deviation of the length of prefabricated beams was distributed in the interval of [−0.46 mm, 5.76 mm] at a 95% confidence level, and [1.43 mm, 4.61 mm] at a 90% confidence level. Compared with the allowable tolerance range [−5 mm, 5 mm] specified in the specification, the maximum and minimum dimensional deviations of the components fully satisfied the requirements of the specification with 90% confidence, at which point the qualification rate reached 100%. However, the minimum dimensional deviation can fully satisfy the requirements with 95% confidence, but the maximum dimensional deviation cannot be satisfied, which is obviously because the lower tolerance limit was too small. The main reason for this is that the center of the tolerance provided by the specification does not match with the center of the size difference in the components.

Table 9. The qualified rates of dimensional deviation under the standards of tolerance.

Type	**Beam**			**Column**			**Wall Slab**			**Composite Floor Slab**	
Project	**Length**	**Width**	**Height**	**Length**	**Width**	**Height**	**Height**	**Width**	**Thickness**	**Length**	**Width**
maximum deviation (mm)	7.18	6.06	8.19	4.78	4.04	8.63	5.08	3.17	6.83	3.11	2.13
Minimum deviation	−0.97	−1.78	−5.14	−9.06	−1.44	−3.65	−7.68	−4.95	−5.08	−6.42	−6.2
Average value (mm)	3.02	1.57	2.45	−2.05	1.34	1.88	−2.39	−1.13	1.81	−2.44	−2.02
Variance	1.91	1.57	3.27	3.74	1.21	4.34	2.91	1.57	4.13	2.21	1.43
Qualification rate (%)	96.80	98.10	94.00	96.20	100.00	93.27	89.78	96.41	95.34	96.71	97.83
Process capability index, C_{pk}						0.55					
Tolerance center deviation, δ (mm)	0.01	0.19	0.57	0.04	0.85	0.78	0.19	0.19	0.19	0.32	0.09
Tolerance, T_0/mm	3.04	1.59	2.67	−1.58	1.75	1.66	−2.23	−1.05	1.05	−2.69	−2.81
Maximum tolerance (mm)	5.25	3.56	5.13	1.63	3.88	5.23	0.98	1.77	4.93	−0.71	−0.89
Minimum tolerance (mm)	0.83	−0.38	0.20	−4.78	−0.39	−1.92	−5.43	−3.86	−2.83	−4.66	−4.73

The values in the existing standards of precast component size tolerances are symmetrical, meaning the upper tolerance limit is equal to the lower tolerance limit. However, the given tolerance requirements have been deemed unsuitable for the current needs of component factory production and inspection. According to the requirements for tolerance values provided by the specifications for the quality acceptance of prefabricated building

components, the quality analysis of prefabricated building components was carried out based on the process capability index under the qualified rate of 90%, using the data shown in Table 9. The tolerance thresholds of different components were thus obtained based on the process capability index.

As can be seen from Table 9, the upper limit of tolerance was not equal to the lower limit of tolerance, which implies asymmetric tolerance, and the center of tolerance did not overlap with the center of distribution. The tolerance interval of the wall slab height was larger than the tolerance interval in the specification, which should lead to tighter control of the wall slab height deviation, while the tolerances relating to other components were smaller than those specified in the specification. The tolerance specified in the specification is thus too conservative, while a tolerance threshold method based on the process capability index can meet the requirements of prefabricated buildings with high precision, thus providing a theoretical basis for the definition of the tolerance threshold of prefabricated components.

5. Conclusions

In response to prevailing standards governing prefabricated buildings, the determination of dimensional tolerances for components is typically empirically undertaken and without a sound theoretical basis. Moreover, traditional measurement methods for prefabricated components are constrained by their limited capacity to measure only a few discrete points on the structure, thereby failing to capture the object's full complexity, particularly in terms of the challenging task of measuring the edge and corner points of concrete structures. The present study proposed a novel method for determining tolerance thresholds based on the process capability index. This approach overcomes the shortcomings of the traditional tolerance division principle, which is based solely on empirical values and results in a mismatch between the tolerance limits and the actual dimensional deviations in component production. To this end, we conducted a comprehensive analysis of over 1400 prefabricated concrete components in China using 3D photogrammetry, and subsequently conducted probabilistic statistical analyses on the geometric parameters of these components. Based on the probability distribution model of dimensional deviation, we studied the tolerance threshold of prefabricated components using the process capability index. Our proposed method presents a rational and accurate solution to determining the tolerances of prefabricated components, thereby paving the way for the development of new standards in the construction industry. The conclusions can be summarized as follows:

1. The range of unqualified random variables for the dimensional geometric parameters of the prefabricated components did not show much diversity, as all values were between 0.99 and 1.02. The coefficients of geometric parameter variation were all below 0.0061, and the component dimensional deviation variability was small. The correlation of dimensional deviation was significant—greater than the significance level of 0.05—and the dimensional deviations of similar components produced by different companies did not show significant differences.
2. The histogram of the frequency distribution of dimensional deviations of prefabricated components decreased from the center to either side, and the fitted curve had only one peak. The component dimensional deviation did not refuse to obey normal or Weibull distribution, but did favor normal distribution.
3. The tolerance center and deviation center of prefabricated components stipulated in Chinese specifications are not consistent. Under the standard tolerance threshold, except for cases in which the height deviation of a prefabricated wall slab is less than 90%, the qualification rate of the dimensional deviation of other components is higher than 90%, and the tolerance thresholds stipulated in the current specifications cannot achieve the required production characteristics of prefabricated components under the current production conditions.
4. A method to determine the dimensional tolerance values of prefabricated components based on the process capability index was proposed. Based on the relationship

between the process capability index and the qualification rate, a process capability index with a 90% qualification rate was determined, and the tolerance values of different components were obtained. This method can meet the requirements of high precision in prefabricated buildings and provide a theoretical basis for the definition of the tolerance of prefabricated components.

However, several limitations of this study must be addressed in future investigations to advance the research in this area. Firstly, the size range of the components involved in the actual project was relatively small, which may limit the generalizability of the findings to other contexts with larger or more complex prefabricated components. Secondly, the quantitative research on the production capacity of prefabricated components is still limited to ordinary prefabricated concrete structures, leaving a research gap related to investigating the production capacity of other types of prefabricated components. Finally, the mathematical fitting model of the process capability index's grading standard needs to be further improved to enhance its accuracy and reliability. To address these limitations, future research could expand the size range of the prefabricated components included in the study and explore the production capacity of different forms and sizes of prefabricated components. Additionally, the further optimization of the fitting parameters of the process capability index, along with establishing an assurance rate for large- and medium-sized prefabricated components, could enhance the accuracy and reliability of the model.

Author Contributions: Conceptualization, H.L. and X.L.; methodology, H.L.; software, J.L.; validation, H.L., X.L. and J.L.; formal analysis, H.L.; investigation, X.L.; resources, H.X.; data curation, H.X.; writing—original draft preparation, H.L.; writing—review and editing, X.L.; visualization, J.L.; supervision, X.L.; project administration, X.L.; funding acquisition, H.L. All authors have read and agreed to the published version of the manuscript.

Funding: This research was funded by the National Natural Science Foundation, grant number 52178179, the Yiyang City Science and Technology Special Funds Project, grant number 2022108, and the Yiyang City Social Science Project, grant number 2023YS172.

Data Availability Statement: The data presented in this study are available on request from the corresponding author. The data are not publicly available due to [3D point cloud data content is too large].

Conflicts of Interest: The authors declare no conflict of interest.

Nomenclature

K_A	geometrical uncertainty
a	actual value of the component size
a_K	design value of the component size
n_i	sample capacity
μ_{K_A}	average of n_i
δ_{K_A}	coefficient of variation
C_{pk}	process capability index
δ	tolerance center deviation value
T_0	tolerance center
η	qualification rate
σ	standard deviation
μ	mean value
T_u	upper tolerance limit
T_l	lower tolerance limit
$\Phi()$	cumulative probability density function
d	tolerance width

References

1. Liu, H.; Chen, J.; Xu, C.; Du, X. Seismic performance of precast column connected with grouted sleeve connectors. *J. Build. Eng.* **2020**, *31*, 101410. [CrossRef]
2. Wang, H.; Zhang, Y.; Gao, W. Life cycle environmental and cost performance of prefabricated buildings. *Sustainability* **2020**, *12*, 2609. [CrossRef]
3. Sacks, R.; Koskela, L.; Dave, B.A.; Owen, R. Interaction of Lean and Building Information Modeling in Construction. *J. Constr. Eng. Manag.* **2010**, *136*, 968–980. [CrossRef]
4. Xu, Z.; Kang, R.; Lu, R. 3D Reconstruction and Measurement of Surface Defects in Prefabricated Elements Using Point Clouds. *J. Comput. Civ. Eng.* **2020**, *34*, 04020033. [CrossRef]
5. Wang, Q.; Tan, Y.; Mei, Z. Computational Methods of Acquisition and Processing of 3D Point Cloud Data for Construction Applications. *Arch. Comput. Methods Eng.* **2019**, *27*, 479–499. [CrossRef]
6. El-Razek, M.E.A.; Bassioni, H.A.; Mobarak, A.M. Causes of Delay in Building Construction Projects in Egypt. *J. Constr. Eng. Manag.* **2008**, *134*, 831–841. [CrossRef]
7. Popovic, P.L.; Arnold, R.C. Preventing Failures of Precast Concrete Facade Panels and Their Connections. In Proceedings of the Second Forensic Engineering Congress, San Juan, PR, USA, 21–23 May 2000; pp. 532–539.
8. Love, P.E.D. Influence of Project Type and Procurement Method on Rework Costs in Building Construction Projects. *J. Constr. Eng. Manag.* **2002**, *128*, 18–29. [CrossRef]
9. Burati, J.L., Jr.; Farrington, J.J. *Construction Industry Institute–Costs of Quality Deviations in Design and Construction*; Clemson University: Clemson, SC, USA, 1987; Volume 29.
10. Liu, P.; Chen, Y.; Luo, X.; Yu, Z.; Long, H. Dimensional Tolerance Control for Prefabricated Building Components. *ACI Struct. J.* **2019**, *116*, 101–114. [CrossRef]
11. Milberg, C.; Tommelein, I.D. Application of tolerance mapping in AEC systems. In Proceedings of the Construction Research Congress 2005: Broadening Perspectives, San Diego, CA, USA, 5–7 April 2005; Volume 233, pp. 1–10.
12. Luo, X.; Long, H.; Dong, S.; Wu, J. Prefabricated Concrete Component Geometry Deviation Statistical Analysis. *Math. Probl. Eng.* **2021**, *2021*, 1–15. [CrossRef]
13. Kim, M.-K.; Cheng, J.C.; Sohn, H.; Chang, C.-C. A framework for dimensional and surface quality assessment of precast concrete elements using BIM and 3D laser scanning. *Autom. Constr.* **2014**, *49*, 225–238. [CrossRef]
14. Kubota, S.; Ho, C.; Nishi, K. Construction and Usage of Three-dimensional Data for Road Structures Using Terrestrial Laser Scanning and UAV with Photogrammetry. *Environ. Sci.* **2019**, 136–143. [CrossRef]
15. Pan, Y.; Dong, Y.; Wang, D.; Chen, A.; Ye, Z. Three-Dimensional Reconstruction of Structural Surface Model of Heritage Bridges Using UAV-Based Photogrammetric Point Clouds. *Remote Sens.* **2019**, *11*, 1204. [CrossRef]
16. Kim, M.; Wang, Q.; Li, H. Non-contact sensing based geometric quality assessment of buildings and civil structures: A review. *Autom. Constr.* **2019**, *100*, 163–179. [CrossRef]
17. Wang, Q.; Kim, M.; Cheng, J.C.; Sohn, H. Automated quality assessment of precast concrete elements with geometry irreg-ularities using terrestrial laser scanning. *Autom. Constr.* **2016**, *68*, 170–182. [CrossRef]
18. Berger, M.; Tagliasacchi, A.; Seversky, L.M.; Alliez, P.; Guennebaud, G.; Levine, J.A.; Sharf, A.; Silva, C.T. A Survey of Surface Reconstruction from Point Clouds. *Comput. Graph. Forum* **2016**, *36*, 301–329. [CrossRef]
19. Huyan, J.; Li, W.; Tighe, S.; Sun, Z.; Sun, H. Quantitative Analysis of Macrotexture of Asphalt Concrete Pavement Surface Based on 3D Data. *Transp. Res. Rec. J. Transp. Res. Board* **2020**, *2674*, 732–744. [CrossRef]
20. Theiler, P.W.; Wegner, J.D.; Schindler, K. Keypoint-based 4-Points Congruent Sets—Automated marker-less registration of laser scans. *ISPRS J. Photogramm. Remote Sens.* **2014**, *96*, 149–163. [CrossRef]
21. Zhang, G.; Chen, C.; Zhang, Y.; Zhao, H.; Wang, Y.; Wang, X. Optimized neural network prediction of interface bond strength for GFRP reinforced cemented soil. *Geomech. Eng.* **2022**, *28*, 599–611.
22. Sun, J.; Aslani, F.; Wei, J.; Wang, X. Electromagnetic absorption of copper fiber oriented composite using 3D printing. *Constr. Build. Mater.* **2021**, *300*, 124026. [CrossRef]
23. Strom, J.; Richardson, A.; Olson, E. Graph-based segmentation for colored 3D laser point clouds. In Proceedings of the 2010 IEEE/RSJ International Conference on Intelligent Robots and Systems, Taipei, Taiwan, 18–22 October 2010; pp. 2131–2136.
24. Czerniawski, T.; Nahangi, M.; Haas, C.; Walbridge, S. Pipe spool recognition in cluttered point clouds using a curvature-based shape descriptor. *Autom. Constr.* **2016**, *71*, 346–358. [CrossRef]
25. Wen, M.; Cho, S.; Chae, J.; Sung, Y.; Cho, K. Range image-based density-based spatial clustering of application with noise clustering method of three-dimensional point clouds. *Int. J. Adv. Robot. Syst.* **2018**, *15*, 1735–1754. [CrossRef]
26. Mao, H.X.; Shi, W.Z. New methodology of representing the positional error of non-point features in GIS. *Int. Arch. Photogramm. Remote Sens. Spat. Inf. Sci.* **2008**, *37*, 1503–1508.
27. de Vasconcellos, R.M.; Campos, F.A.; Maestrini, S.R. Response variability in reinforced concrete structures with un-certain geometrical and material properties. *Nucl. Eng. Des.* **2003**, *226*, 205–220. [CrossRef]
28. Wattimanela, H.J. Analysis of Types of Foreshock and Aftershock Earthquake Distributions in 2018 in Lombok Island Based on Depth Using the Kolmogorov-Smirnov and Chi-Squared Test Approaches. *AIP Conf. Proc.* **2023**, *2588*, 050008.
29. Lanzante, J.R. Testing for differences between two distributions in the presence of serial correlation using the Kolmogo-rov–Smirnov and Kuiper's tests. *Int. J. Climatol.* **2021**, *41*, 6314–6323. [CrossRef]

30. Bazant, Z.P.; Xi, Y.; Reid, S.G. Statistical size effect in quasi-brittle structures: I. Is Weibull theory applicable. *J. Eng. Mech.* **1991**, *117*, 2609–2622. [CrossRef]
31. Vu, C.-C.; Ho, N.-K.; Pham, T.-A. Weibull statistical analysis and experimental investigation of size effects on the compressive strength of concrete-building materials. *Case Stud. Constr. Mater.* **2022**, *17*, 1231–1248. [CrossRef]
32. *DIN 18202-1997*; Tolerances for Building Structures. Deutscher Verband für Industrienormen: Berlin, Germany, 1997.
33. *DIN 18202-2005*; Tolerances in Building Construction—Buildings. Deutscher Verband für Industrienormen: Berlin, Germany, 2005.
34. *I.S. EN 13369:2018*; Common Rules for Precast Concrete Products. British Standards Institution: London, UK, 2004.
35. Wilden, H. *PCI Design Handbook Precast and Prestressed Concrete*; Precast/Prestressed Concrete Institute: Chicago, IL, USA, 2010.
36. *JGJ1-2014*; Technical Specification for Precast Concrete Structures. China Institute of Building Standards: Beijing, China, 2014.
37. *GB/T 50204-2015*; Code for Quality Acceptance of Concrete Structure Construction. China Academy of Building Research: Beijing, China, 2015.
38. *GB/T 51231-2016*; Technical Standard for Assembled Buildings with Concrete Structure. China Academy of Building Research: Beijing, China, 2016.
39. Kotz, S.; Johnson, N.L. Process capability indices. *Chapman Hall/CRC* **2017**, *231*, 409–422.
40. Yang, Y.; Liu, Z.; Tang, H.; Peng, J. Deflection-based failure probability analysis of low shrinkage-creep concrete structures in presence of non-stationary evolution of shrinkage and creep uncertainties. *Constr. Build. Mater.* **2023**, *376*, 131077. [CrossRef]
41. Pearn, W.L.; Chen, K.-S. Making decisions in assessing process capability indexCpk. *Qual. Reliab. Eng. Int.* **1999**, *15*, 321–326. [CrossRef]

Disclaimer/Publisher's Note: The statements, opinions and data contained in all publications are solely those of the individual author(s) and contributor(s) and not of MDPI and/or the editor(s). MDPI and/or the editor(s) disclaim responsibility for any injury to people or property resulting from any ideas, methods, instructions or products referred to in the content.